

Electronic Supporting Information

Impact of Nuclearity and Topology on the Single Molecule Magnet Behaviour of Hexaazatrinaphthylene-Based Cobalt Complexes

Maykon A. Lemes,^a François Magnan,^a Bulat Gabidullin,^a and Jaclyn L. Brusso^{*a}

^aDepartment of Chemistry and Biomolecular Sciences, University of Ottawa, Ontario K1N 6N5, Canada.

Contents (9 pages)

Page S2	Crystallographic data
Page S5	Magnetic measurements
Page S9	References

Table S1 – Crystallographic data for complexes **1** and **2**.

	1	2
Empirical formula	C ₃₄ H ₁₄ CoF ₁₂ N ₆ O ₄	C ₄₄ H ₁₆ Co ₂ F ₂₄ N ₆ O ₈
Formula weight	942.37	1422.62
Crystal system	Triclinic	Monoclinic
Space group	P-1	P2 ₁ /c
<i>a</i> /Å	8.1562 (4)	18.2906 (7)
<i>b</i> /Å	11.3461 (5)	9.6629 (4)
<i>c</i> /Å	20.3012 (8)	31.6337 (13)
$\alpha/^\circ$	86.491 (3)	90
$\beta/^\circ$	88.276 (3)	97.5890(10)
$\gamma/^\circ$	75.154 (3)	90
<i>V</i> / Å ³	1812.37	5541.98
<i>Z</i>	2	4
<i>T</i> /K	200	200
<i>D_{Calc}</i> /Mg m ⁻³	1.727	1.705
μ/mm^{-1}	0.733	0.739
Θ range for data collect.	1.86 to 27.75°	1.60 to 28.28°
Reflections collected/unique	21286/8520	65591/13592
Goodness-of-fit on <i>F</i> ²	1.004	1.019
R1,wR2 (>2σ(I))	0.0602, 0.1462	0.0443, 0.1181

Table S2 – Selected bond lengths (Å) for **1** and **2**.

1	2
Co(1)-O(4)	2.011(3)
Co(1)-O(1)	2.053(3)
Co(1)-O(2)	2.083(3)
Co(1)-O(3)	2.109(3)
Co(1)-N(1)	2.158(3)
Co(1)-N(6)	2.169(3)
	Co(1)-O(1)
	2.0265(16)
	Co(1)-O(4)
	2.0444(16)
	Co(1)-O(3)
	2.0531(17)
	Co(1)-O(2)
	2.0848(15)
	Co(1)-N(1)
	2.1673(19)
	Co(1)-N(2)
	2.1864(17)
	Co(2)-O(5)
	2.0416(16)
	Co(2)-O(8)
	2.0416(16)
	Co(2)-O(6)
	2.0702(16)
	Co(2)-O(7)
	2.0817(16)
	Co(2)-N(4)
	2.1699(18)
	Co(2)-N(3)
	2.1896(17)

Table S3 – Selected angles ($^{\circ}$) for **1** and **2**.

	1		2
O(4)-Co(1)-O(1)	172.37(11)	O(1)-Co(1)-O(4)	174.59(6)
O(4)-Co(1)-O(2)	95.99(11)	O(1)-Co(1)-O(3)	91.95(7)
O(1)-Co(1)-O(2)	85.74(11)	O(4)-Co(1)-O(3)	86.81(7)
O(4)-Co(1)-O(3)	85.53(11)	O(1)-Co(1)-O(2)	87.26(6)
O(1)-Co(1)-O(3)	87.36(11)	O(4)-Co(1)-O(2)	87.35(7)
O(2)-Co(1)-O(3)	82.23(11)	O(3)-Co(1)-O(2)	82.60(7)
O(4)-Co(1)-N(1)	85.69(11)	O(1)-Co(1)-N(1)	96.22(7)
O(1)-Co(1)-N(1)	101.53(11)	O(4)-Co(1)-N(1)	85.60(7)
O(2)-Co(1)-N(1)	96.41(11)	O(3)-Co(1)-N(1)	169.83(7)
O(3)-Co(1)-N(1)	170.92(11)	O(2)-Co(1)-N(1)	103.78(7)
O(4)-Co(1)-N(6)	98.36(11)	O(1)-Co(1)-N(2)	85.99(6)
O(1)-Co(1)-N(6)	81.05(10)	O(4)-Co(1)-N(2)	99.40(6)
O(2)-Co(1)-N(6)	163.67(11)	O(3)-Co(1)-N(2)	97.56(6)
O(3)-Co(1)-N(6)	106.57(11)	O(2)-Co(1)-N(2)	173.25(6)
N(1)-Co(1)-N(6)	77.02(11)	N(1)-Co(1)-N(2)	77.05(6)
		O(5)-Co(2)-O(8)	175.23(6)
		O(5)-Co(2)-O(6)	86.67(6)
		O(8)-Co(2)-O(6)	90.31(6)
		O(5)-Co(2)-O(7)	90.52(7)
		O(8)-Co(2)-O(7)	85.41(7)
		O(6)-Co(2)-O(7)	82.31(7)
		O(5)-Co(2)-N(4)	102.09(7)
		O(8)-Co(2)-N(4)	82.09(6)
		O(6)-Co(2)-N(4)	100.90(7)
		O(7)-Co(2)-N(4)	167.10(7)
		O(5)-Co(2)-N(3)	85.11(6)
		O(8)-Co(2)-N(3)	98.14(6)
		O(6)-Co(2)-N(3)	170.88(7)
		O(7)-Co(2)-N(3)	101.69(6)
		N(4)-Co(2)-N(3)	77.03(6)

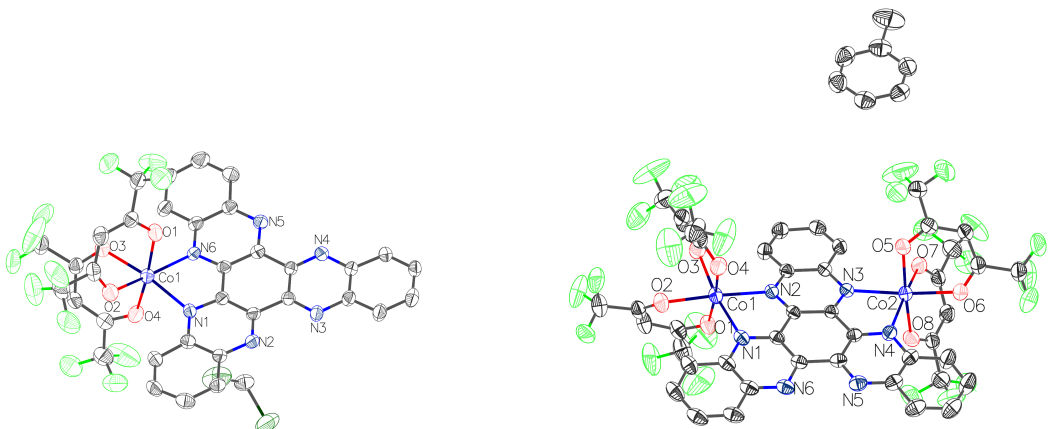


Figure S1. Thermal ellipsoid drawings of $[\text{Co}^{\text{II}}(\text{HATN})(\text{hfac})_2] \cdot (\text{CH}_2\text{Cl}_2)$ (**1**, left) and $[\text{Co}^{\text{II}}_2(\text{HATN})(\text{hfac})_4] \cdot (\text{PhCH}_3)$ (**2**, right).

Table S4 – Results from Shape Analysis for $[\text{Co}^{\text{II}}(\text{HATN})(\text{hfac})_2] \cdot (\text{CH}_2\text{Cl}_2)$ (1**) and $[\text{Co}^{\text{II}}_2(\text{HATN})(\text{hfac})_4] \cdot (\text{PhCH}_3)$ (**2**).**

Structure ML_6	Metal Centre	HP-6	PPY-6	OC-6	TPR-6	JPPY-6
$\text{Co}^{\text{II}}(\text{HATN})(\text{hfac})_2$	Co1	27.828	21.032	1.800	10.495	24.344
$\text{Co}^{\text{II}}_2(\text{HATN})(\text{hfac})_4$	Co1	27.882	23.391	1.171	12.518	26.486
	Co2	27.324	23.043	1.488	13.114	26.148

HP-6: D6h, Hexagon; PPY-6: C5v, Pentagonal pyramid; OC-6: Oh, Octahedron; TPR-6: D3h, Trigonal prism; JPPY-6: C5v, Johnson pentagonal pyramid J2

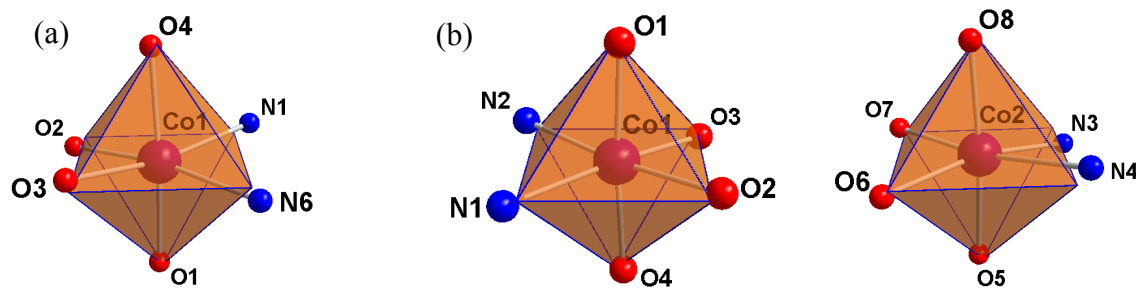


Figure S2. Deviation from ideal octahedral environment about the Co^{II} ions in (a) $[\text{Co}^{\text{II}}(\text{HATN})(\text{hfac})_2] \cdot (\text{CH}_2\text{Cl}_2)$ and (b) $[\text{Co}^{\text{II}}_2(\text{HATN})(\text{hfac})_4] \cdot (\text{PhCH}_3)$.

Magnetic Measurements

The magnetic susceptibility data for compounds **1** and **2** were fit using the PHI program.¹ The spin Hamiltonians used were modified versions of a reported fitting model.² The magnetic susceptibility data for compound **1** was fit using the spin-Hamiltonian shown below.

$$\hat{H} = D \left(S_Z^2 - \frac{1}{3} \vec{S}^2 \right) + \mu_B g \vec{S} H$$

Where the first term represents the axial zero-field D , assuming parallel anisotropic tensors for one Co^{II} ion; the second term represents the Zeeman interaction; μ_B = Bohr magneton; g = Lande factors or g factors; and H = Magnetic field.

For compound **2**, the magnetic susceptibility data was fit using the spin-Hamiltonian shown below using -2J formalism.

$$\hat{H} = -2J(\vec{S}_1 \cdot \vec{S}_2) + D \left(\sum_{i=1}^2 \left(S_{iz}^2 - \frac{1}{3} \vec{S}_i^2 \right) \right) + \mu_B g \left(\sum_{i=1}^2 \vec{S}_i \right) H + \sum_{i=1}^N \lambda_i (\sigma_i \vec{L}_i \cdot \vec{S}_i)$$

Where the first term represents the isotropic exchange interactions for $S_1=S_2=3/2$; the second term represents the axial zero-field D , assuming parallel anisotropic tensors for two Co(II) ions; the third term represents the Zeeman interaction; the fourth term represents the spin-orbit coupling; μ_B = Bohr magneton; g = Lande factors or g factors; H = Magnetic field; λ_i = spin-orbit constant; and σ_i = Orbital reduction parameter.

Table S5 – Parameters and results from the fit of dc measurements applied for compound **1** using four different models. The bold blue numbers indicate the parameters fixed during the process of fitting, the values used are based on the previous fitting, while the unbolted black parameters were left to vary.

Parameters	I	II	III	IV
D/hc (cm ⁻¹)	60	60	- 60	-60
g	1.84	2.06	2.06	1.64
λ (cm ⁻¹)	- 67	- 11	-158	-50

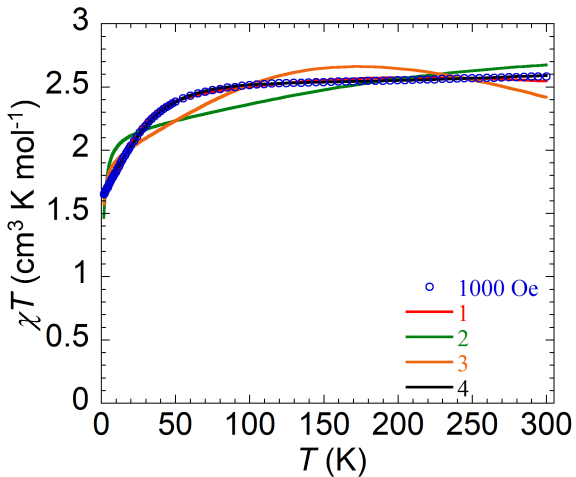


Figure S3 – χT vs. T plot of the comparison between different fitting procedures applied in the experimental magnetic dc data of compound **1**. The blue circles indicate the experimental data while the red (I), green (II), orange (III) and black (IV) lines represent the fit obtained according to Table 1

Table S6 – Parameters and results from the fit of dc measurements applied for compound **1** using two different models only considering S , g and D . The bold blue numbers indicate the parameters fixed during the process of fitting, the values used are based on the previous fitting, while the unbolted black parameters were left to vary.

Parameters	V	VI
D/hc (cm^{-1})	-60	60
g	2.06	1.84

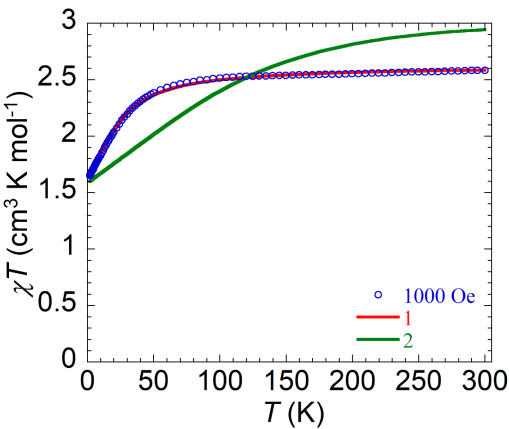


Figure S4 – χT vs. T plot of the comparison between different fitting procedures applied in the experimental magnetic dc data of compound **1**. The blue circles indicate the experimental data while the red (V) and green (VI) lines represent the fit obtained according to Table 2.

Table S7 – Parameters and results from the fit of magnetic susceptibility applied for compound **2** using four different models. The bold numbers indicate the parameters let fix during the process of fitting, the values used are based on the previous fitting, while the unbolded black parameters were left to vary.

Parameters	I	II	III	IV
J/hc (cm ⁻¹)	- 0.1	- 0.1	- 0.1	- 0.1
D/hc (cm ⁻¹)	- 20.38	- 20.38	20.38	20.38
g	1.81	2.12	2.12	2.22
λ (cm ⁻¹)	-31	-131	-130	-1.13

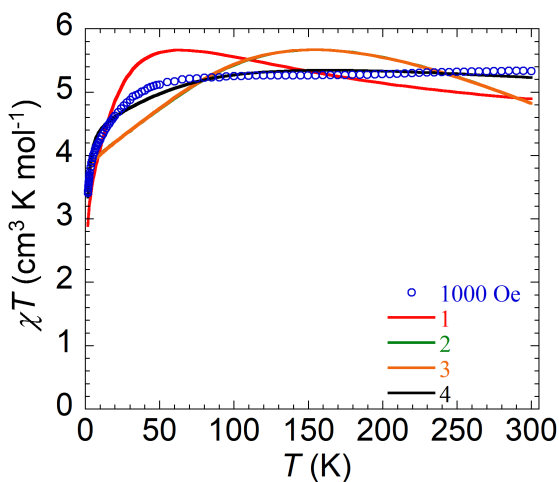


Figure S5 – χT vs. T plot of the comparison between different procedures of fitting the experimental magnetic dc data of compound **2**. The blue circles indicate the experimental data while red (I), green (II), orange (III) and, black (IV) lines represent the fit obtained according to the data in Table 3.

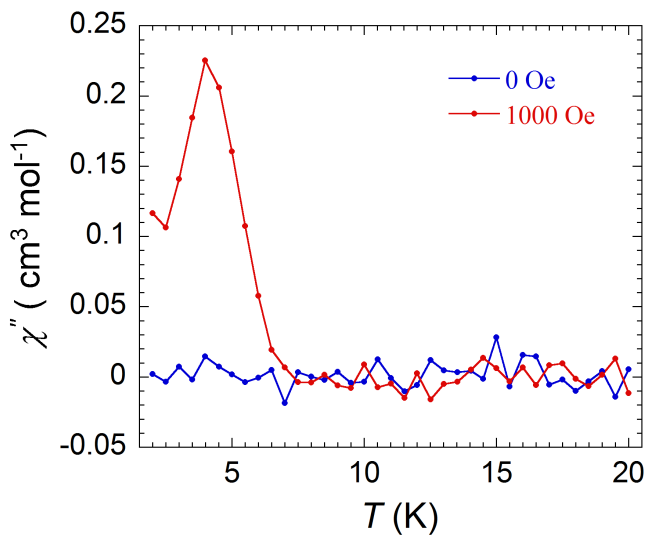


Figure S6 – Out-of-phase plot (χ'') for the ac check measurements of **1** under 0 Oe applied field and 1000 Oe.

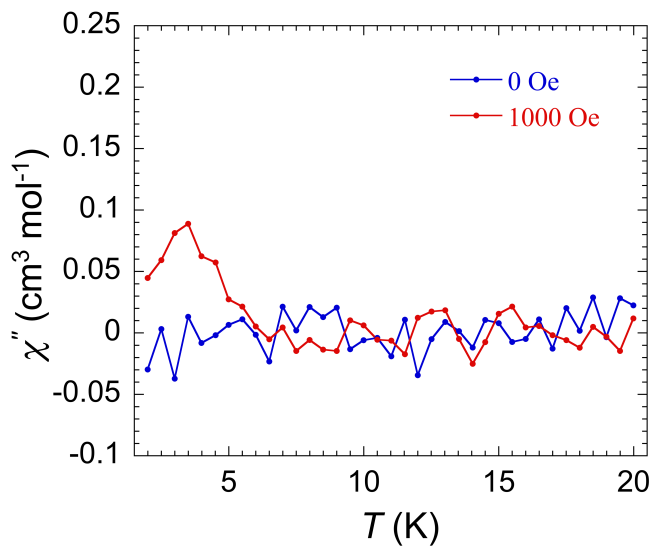


Figure S7 – Out-of-phase plot (χ'') for the ac check measurements of **2** under 0 Oe applied field and 1000 Oe.

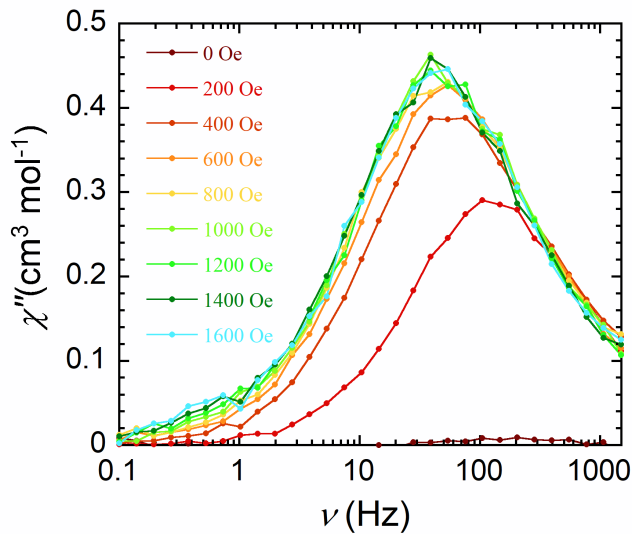


Figure S8 – Out-of-phase plot (χ'') of **1** measured under static fields from 200 Oe to 1600 Oe at 1.8K.

Table S8 – Parameters obtained by fitting the temperature dependence of the magnetization times (τ) using the multi-relaxation processes model (eq.1).

$$\tau^{-1} = \tau_0^{-1} e^{-U_{eff}/K_B T} + AB^m T + CT^n \quad (\text{eq. 1})$$

Parameters	Values
τ_0^{-1}, s	$2.63 \cdot 10^{-6}$
U_{eff}, K	18.38
$C, s^{-1} K^{-n}$	13
n	4
$A, T^{-m} K^{-1} s^{-1}$	$-2.98 \cdot 10^5$
B_{dc}, T	0.06
m	9

References

1. N. F. Chilton, R. P. Anderson, L. D. Turner, A. Soncini and K. S. Murray, *J. Comp. Chem.*, 2013, **34**, 1164-1175.
2. D. I. Alexandropoulos, B. S. Dolinar, K. R. Vignesh and K. R. Dunbar, *J. Am. Chem. Soc.*, 2017, **139**, 11040-11043.